Towards a formalism for mapping the spacetimes of massive compact objects: Bumpy black holes and their orbits

Nathan A. Collins and Scott A. Hughes
Department of Physics, Massachusetts Institute of Technology, 77 Massachusetts Ave., Cambridge, Massachusetts 02139, USA
(Received 13 February 2004; published 25 June 2004)

Astronomical observations have established that extremely compact, massive objects are common in the Universe. It is generally accepted that these objects are, in all likelihood, black holes. As observational technology has improved, it has become possible to test this hypothesis in ever greater detail. In particular, it is or will be possible to measure the properties of orbits deep in the strong field of a black hole candidate (using x-ray timing or future gravitational-wave measurements) and to test whether they have the characteristics of black hole orbits in general relativity. Past work has shown that, in principle, such measurements can be used to map the spacetime of a massive compact object, testing in particular whether the object's multipolar structure satisfies the rather strict constraints imposed by the black hole hypothesis. Performing such a test in practice requires that we be able to compare against objects with the ''wrong'' multipole structure. In this paper, we present tools for constructing the spacetimes of *bumpy black holes*: objects that are *almost* black holes, but that have some multipoles with the wrong value. In this first analysis, we focus on objects with no angular momentum. Generalization to bumpy Kerr black holes should be straightforward, albeit labor intensive. Our construction has two particularly desirable properties. First, the spacetimes which we present are good deep into the strong field of the object—we do not use a ''large r'' expansion (except to make contact with weak field intuition). Second, our spacetimes reduce to the exact black hole spacetimes of general relativity in a natural way, by dialing the ''bumpiness'' of the black hole to zero. We propose that bumpy black holes can be used as the foundation for a null experiment: if black hole candidates are indeed the black holes of general relativity, their bumpiness should be zero. By comparing the properties of orbits in a bumpy spacetime with those measured from an astrophysical source, observations should be able to test this hypothesis, stringently testing whether they are in fact the black holes of general relativity.

DOI: 10.1103/PhysRevD.69.124022 PACS number(s): 04.25.Nx, 04.30.Db, 04.70.Bw

I. INTRODUCTION

A. Motivation

Observations have now established that the cores of nearly all nearby galaxies contain a massive, compact, dark object [1,2]. These objects range in mass from several $10^5 M_\odot$ to several $10^9 M_\odot$. Extremely compact stellar mass objects ($\sim 10 M_\odot$ or so) exist and have been studied in the galactic field (see, e.g., Ref. [3] for a review). Evidence suggests the existence of objects with intermediate masses, $10^2 M_\odot - 10^4 M_\odot$, filling the gap between the supermassive and stellar mass objects (see, e.g., Ref. [4] for a review). The most generally accepted explanation is that these compact bodies are massive black holes.

Although this is the most generally accepted explanation for these objects, it is not the only explanation. In some cases, the massive dark objects seen in galaxy cores can be explained quite well as dense clusters of stars or stellar remnants. Such models are rapidly becoming disfavored in many cases as our ability to study the central regions of galaxies improves—many of these putative clusters would have to be so compact that they would not be gravitationally stable. By using ''exotic'' matter, it becomes possible to build objects that are massive, compact, but stable. For example, by tuning the mass and self interaction of a massive scalar field [5,6], one can build an object that is consistent with much of the observational evidence available today. Indeed, the fields that describe some of these black hole alternatives are similar to some dark matter candidates, leading to the suggestion that massive compact objects could be dark matter condensates rather than black holes.

Other recently proposed black hole alternatives are motivated by a desire to avoid the information paradox—the loss of information through the black hole's event horizon. Such models find ways of eliminating the event horizon altogether, for instance by replacing the event horizon with a hard surface surrounding a ball of negative energy density (the ''gravastar'' model) [7], or by postulating that spacetime itself undergoes a phase transition in the presence of very strong gravitational fields [8]. If such objects exist in nature, they should have a deep, strong field structure very different from that of black holes [9].

Astronomical measurements are now becoming able to probe into the very strong field of compact objects: optical and infrared observations track stellar orbits at the core of the Milky Way, probing the spacetime of the presumed black hole at Sgr A* [11,12]; x-ray observations of quasi-periodic oscillations from black hole candidates carry information about gas in the hole's deep strong field [13]; and future gravitational-wave observations may be able to track the sequence of orbits followed by a compact body that slowly spirals into a massive black hole (an ''extreme mass ratio binary,'' in which the compact body is far less massive than the black hole) [14,15]. The question of whether these objects are truly the black holes of general relativity or are described by some alternative model reduces to the question of how one may use measurements of orbital properties to map the spacetime structure (i.e., the gravitational field) of

these objects [16]. One thus needs to be able to relate the properties of the measured orbits to the structure of the central gravitating objects. A powerful way of doing this is by a multipole expansion of the compact object's spacetime.

B. Multipoles of massive compact objects

In Newtonian theory, the gravitational field of a body is simply described by expanding the potential in spherical harmonics. The potential Φ must satisfy

$$\nabla^2\Phi = 4\pi G\rho \quad \text{(interior)},$$
$$= 0 \quad \text{(exterior)}. \tag{1.1}$$

In the exterior, the potential may be expanded as

$$\Phi = -G\sum_{lm} \frac{M_{lm}Y_{lm}}{r^{l+1}}. \tag{1.2}$$

By matching to an expansion of the interior solution and enforcing Eq. (1.1), we see that the coefficients M_{lm} are *mass multipole moments*: numbers that describe the angular distribution of matter inside the star. For simplicity, let us focus for a moment on axially symmetric objects, so that only $m=0$ matters. Then, for example, $M_{00}=M$, the total mass of the object. By an appropriate choice of the center of our coordinate system, we put the moment $M_{10}=0$. The first interesting moment is M_{20}, the quadrupole moment of the object. This moment has the form $\mathcal{Q}ML^2$, where L is the object's ''size'' (e.g., its mean radius), and the dimensionless number $\mathcal{Q}$ describes the quadrupolar deformation. Higher moments can likewise be interpreted as l-polar moments of the mass distribution. Because these moments directly determine the gravitational potential outside of the gravitating object, one can measure properties of its mass distribution by measuring the ''shape'' of the gravitational potential. Doing so by studying the properties of satellite orbits is the science of *geodesy*.

Somewhat remarkably, such a description describes the exterior spacetimes of bodies in general relativity as well. For any gravitating body that is stationary, axisymmetric, and reflection symmetric across the equator—encompassing black holes plus a wide variety of perturbations—the exterior spacetime is fully specified by a pair of multipole moment families: the mass multipole moment M_l, plus the *current* multipole moment S_l [17,18]. (Since we have restricted ourselves to axisymmetry, we only consider $m=0$. We henceforth drop this subscript.) The current moment S_l does not appear in Newtonian theory; it reflects the fact that mass and energy flows gravitate in general relativity. For example, the moment S_1 is the magnitude of the spin angular momentum of the body.

If the gravitating body is a Kerr black hole, then the values of the mass and current moments are strongly restricted: in units in which $G=1$, $c=1$ (which we use throughout this paper), we must have [18]

$$M_l + iS_l = M(ia)^l. \tag{1.3}$$

This equation tells us that $M_0=M$, the total mass of the Kerr black hole, and $S_1=aM$, the magnitude of the black hole's spin angular momentum in these units—precisely what we already expect. More interestingly, *all* higher moments are completely determined by these two values. The exterior spacetime of a Kerr black hole is completely determined by its two lowest multipole moments—its mass and spin.

This is nothing more than a restatement of the ''no hair'' theorem [19–22]. By analogy with geodesy, this suggests that one can test the no hair theorem by measuring orbits near black holes. Using a spacetime that does not necessarily assume the Kerr form of the moments, one could then determine M_l and S_l. If that object is in fact a black hole as described by general relativity, the only free moments are those for $l=0$ and $l=1$. Once they have been determined, *all* higher moments are constrained via Eq. (1.3). Such ''geodesy for black holes'' (which has been given the names ''bothrodesy'' and ''holiodesy'' [23]) would provide a stringent test of the black hole nature of massive compact objects in the universe.

The first detailed analysis of how one might be able to falsify the black hole nature of a massive compact object was by Fintan Ryan [24]. Ryan showed how to build the spacetime of an object with arbitrary multipole structure, and then analyzed the orbits of small bodies in that spacetime. (''Small'' means that these bodies do not themselves significantly distort the spacetime, and so can be treated as following approximately geodesic trajectories.) His analysis demonstrated that the accumulated orbital phase was sensitive to these multipoles. Orbital phase (or some surrogate of this phase) is directly observed by, for example, x-ray timing (today) and gravitational-wave detectors (future). One could thus imagine using measurements of accumulated orbital phase to test the black hole nature of a massive compact object. Focusing on gravitational-wave measurements with the planned space-based laser interferometer LISA [25], Ryan showed that enough multipoles should be measurable to easily falsify the black hole hypothesis. In many cases, enough multipoles would be measurable (up to $l\sim 5$ or 6) to stringently constrain the object's black hole nature [26].

Unfortunately, the multipole expansion used by Ryan does not work very well in the deep strong fields of massive black holes, where one expects orbital phases to most stringently test the black hole hypothesis. (In considering applications to both x-ray timing and extreme mass ratio binary gravitational-wave sources, it should be noted that the most interesting radiation is generated at very small radii. X-ray emission from a disk comes from gas very close to the innermost stable orbit; extreme mass ratio binaries spend of order one year spiraling through the hole's very strong field before reaching the innermost orbits and plunging through the horizon.) Multipole moments essentially label different powers of a $1/r$ expansion. In the strong field of a black hole (small r), such an expansion is not going to be very useful [27]. The in-utility of this expansion is reflected by the extremely large number of terms that must be kept to describe a spacetime with arbitrary multipole moments at small radius (cf. Ref. [24], Sec. III).

C. Bumpy black holes

We advocate a different approach. The reason for introducing a multipolar expansion is to describe a candidate spacetime differing from that of a black hole. If one accepts as a starting point the idea that the black hole hypothesis *probably* describes the massive compact objects in question, then one just needs a spacetime to compare against that differs *slightly* from that of a black hole. Our goal is then to set up a null experiment: we find a trial spacetime that exhibits slight deviations from the spacetime of a black hole. If the black holes of nature are the black holes of general relativity, we will measure the deviation to be zero.

Past work on candidate objects to test the black hole hypothesis has focused primarily on boson and soliton stars [6,26]. Though of great intrinsic interest, there is no natural way for a boson star spacetime to smoothly limit to the spacetime of a black hole. If the massive compact objects we observe in the universe are in fact black holes, then tests based on the boson star model will not provide useful constraints on orbit observations. As a ''straw man'' for the black hole hypothesis, boson stars may unfortunately contain too much straw.

We advocate instead the use of *bumpy black holes*: objects that have a multipolar structure that is very nearly, but not quite, that of a black hole. As the name suggests, these are black holes with small bumps on them. If the universe's observed massive compact objects are in fact black holes, then we will find that the amplitude of these bumps is zero (within measurement uncertainty). A bumpy black hole should be a trial spacetime that behaves well deep into the strong field, and that exhibits a *controllable* deviation from the Kerr solution. In particular, these trial spacetimes should reduce to normal black holes when the deviation is set to zero—bumpy black holes become normal black holes when the bumps are removed. This reduction to normal black holes is a crucial element of using bumpy black holes as a basis for a null experiment.

A key piece of our guiding philosophy is that the notion of multipoles is most useful in the weak field of an object. One should not be too attached to multipole moments if the goal is an analysis that applies to strong gravitational fields. Of course, by taking the weak field (large r) limit of the spacetimes we construct, bumpy black holes are very usefully described using multipoles. Indeed, the goal of our detailed calculations will be to assemble a perturbation that is purely quadrupolar when examined in the weak field. Our construction, however, works very well deep in the strong field, which is crucial for applying these notions to observations.

An important question to ask at this point is *how* one can build a stationary spacetime corresponding to a bumpy black hole. A key portion of the proof of the no hair theorem demonstrates that any deformation to a black hole will tend to radiate very quickly, removing the bump and pushing us back to the Kerr black hole solution [21,22]. Some mechanism must exist to maintain the bump. This is likely to require unphysical matter; the example which we describe in fact requires naked singularities. One might object that a bumpy black hole spacetime is thus, by construction, unphysical. Our viewpoint is that the physicality of these spacetimes is *irrelevant*. Our goal in this analysis is *not* to build a spacetime which might conceivably exist in nature. Instead, we wish to build a black hole straw man with just the right amount of straw to probe the nature of massive compact objects.

D. Overview of this paper

The goal of this paper is to present the bumpy black hole concept, to show how bumpy black hole spacetimes are generated, and to demonstrate that the magnitude of the bumps is encoded in the accumulated phase of the hole's orbits. We focus upon axisymmetric distortions of black holes—even in axisymmetry, an incorrect moment is enough to falsify the black hole hypothesis for a massive compact object.

We have argued that the language of multipoles is not useful for describing an object's strong field orbits. To substantiate this argument, we review the multipole description of spacetimes and their orbits in Sec. II, summarizing the key results of Ryan [24]. Ryan's formulas and the detailed description of the spacetime in the multipole language show that, as we try to characterize the massive object's strong field, the description becomes extremely complicated. Although it is possible in principle to use this description to develop tools for mapping spacetimes, it does not appear to be the best approach in practice.

We then begin our detailed presentation of bumpy black holes. In Sec. III, we show how to build a bumpy black hole spacetime. The spacetime of a stationary, axisymmetric object is fully described by the Weyl metric [28],

$$ds^2 = -e^{2\psi}dt^2 + e^{2\gamma-2\psi}(d\rho^2+dz^2) + e^{-2\psi}\rho^2 d\phi^2. \tag{1.4}$$

Our strategy is to pick an exact solution $\psi=\psi_0(\rho,z)$, $\gamma=\gamma_0(\rho,z)$ for which the line element (1.4) describes a black hole. For this first analysis, we specialize our background to Schwarzschild black holes; generalization to Kerr black holes should be straightforward in principle (though it may be somewhat involved algebraically). We then use this exact solution as a background against which to introduce a perturbation, putting $\psi=\psi_0+\psi_1$ and requiring $\psi_1/\psi_0 \ll 1$; a similar perturbation is defined for γ. The perturbations are constrained by the requirement that they satisfy the vacuum Einstein equations, expanded to first order.

This formulation of the metric is particularly useful because the function ψ reduces to the Newtonian gravitational potential of the source in the weak field. We therefore choose our perturbation ψ_1 in such a manner that the weak-field perturbation can be thought of as changing the source's multipoles *as measured in the weak field*. We then solve the linearized Einstein equations in order to specify the perturbation throughout the exterior spacetime of the bumpy black hole.

Before specifying our perturbations, we first examine the properties of orbits in the bumpy hole's equatorial (reflection symmetry) plane (Sec. IV). Many useful quantities can be computed in terms of the perturbations ψ_1 and γ_1—the orbit's energy E, angular momentum L, and the location of the

last stable orbit (a separatrix in orbital phase space dividing dynamically stable and unstable orbits). We also write down an equation describing the differential advance of the orbit's periapsis. The periapsis shift arises from a mismatch between the radial and azimuthal orbital frequencies; as such, it can be a sensitive probe of the spacetime. Deviations of this shift from the canonical Schwarzschild value encode the black hole's bumpiness.

We choose particular perturbations in Secs. V and VI. A very simple and useful one is that of a point mass near the black hole. We build a bumpy black hole in Sec. V by placing a pair of point masses with mass $\mu/2$ each near the hole's ''north'' and ''south'' poles. The same system was used by Suen, Price, and Redmount (SPR) [29] to set up an analysis of a black hole with a deformed event horizon. Our analysis is similar to that of SPR, though we do not focus on the region of spacetime near the horizon. We build a second type of bumpy black hole in Sec. VI by placing a ring of mass μ about the hole's equator.

As the analysis of Secs. V and VI shows, both the polar point mass and the equatorial ring do indeed change the metric's quadrupole moment. We demonstrate this by calculating weak-field periapsis precession in these spacetimes and showing that the shift contains a term which is exactly what we expect for weak-field quadrupolar distortions (computed in Appendix A). Unfortunately, these perturbations also change the metric's *monopole* moment (i.e., its mass). Fortunately, we can build a purely quadrupolar distortion by combining *negative* mass polar points with a positive mass equatorial ring, or vice versa. (Bearing in mind that our goal is to build trial spacetimes for testing the black hole hypothesis, the unphysicality of a negative perturbing mass is not a concern.) In Sec. VII A, we show that the weak-field periapsis precession with this combined mass distribution is identical to that of a Schwarzschild black hole plus a quadrupolar deformation. The points + ring perturbation to a Schwarzschild black hole thus perfectly matches our requirements for a bumpy black hole. We investigate the strong-field character of this spacetime in Sec. VII B, showing in particular that the hole's bumpiness is usefully encoded in the strong-field periapsis precession.

Concluding discussion is given in Sec. VIII. In particular, we outline further work that should be done to connect the bumpy black hole concept to future astrophysical observations. Chief among the tasks needed is a generalization to Kerr black hole backgrounds; some steps in this direction are outlined in Appendix B.

II. METRICS AND MULTIPOLE MOMENTS: AN OVERVIEW

As stated in the Introduction, one can build a spacetime by specifying a set of mass and current multipole moments (M_l, S_l). In actuality, one builds a spacetime from a set of coefficients a_{jk} which determine orbital characteristics; the multipole moments can then be extracted from these coefficients. In this section we briefly describe the details of this analysis, and discuss why we believe this is not the most effective way to map black hole spacetimes in practice. Much of our presentation is essentially a synopsis of Fintan Ryan's calculation; see Ref. [24] for detailed discussion.

To begin, we must pick a spacetime sufficiently general to encompass the stationary, axisymmetric sources we wish to describe. Ryan begins with the line element

$$ds^2 = -F(dt-\omega d\phi)^2 + \frac{1}{F}[e^{2\gamma}(d\rho^2+dz^2)+\rho^2 d\phi^2]. \tag{2.1}$$

The functions F, γ, and ω depend on ρ and $|z|$. The radial coordinate ρ labels displacement from the source's symmetry axis; z labels displacement above or below the source's ''equatorial'' plane. By construction, the spacetime is stationary and axisymmetric (F, γ, and ω do not depend on t or ϕ), and is reflection symmetric about the equatorial plane (dependence on $|z|$).

For an axial and reflection symmetric spacetime, the metric functions F, γ, and ω can be generated from the *Ernst potential* $\mathcal{E}$. This function and a related complex function $\tilde{\xi}$ are defined via

$$\mathcal{E} = F + i\Psi = \frac{\sqrt{\rho^2+z^2}-\tilde{\xi}}{\sqrt{\rho^2+z^2}+\tilde{\xi}}, \tag{2.2}$$

where the function Ψ is related to ω by

$$\omega(\rho,z) = -\int_\rho^\infty \left(\frac{\rho'}{F^2}\frac{\partial\Psi}{\partial z}\right) d\rho'. \tag{2.3}$$

The quantity in parentheses under the integral is evaluated at constant z. The function γ can be determined once F and ω are known: the vacuum Einstein equations tell us

$$\frac{\partial\gamma}{\partial\rho} = \frac{1}{4}\frac{\rho}{F^2}\left[\left(\frac{\partial F}{\partial\rho}\right)^2 - \left(\frac{\partial F}{\partial z}\right)^2\right] - \frac{1}{4}\frac{F^2}{\rho}\left[\left(\frac{\partial\omega}{\partial\rho}\right)^2 - \left(\frac{\partial\omega}{\partial z}\right)^2\right], \tag{2.4}$$

$$\frac{\partial\gamma}{\partial z} = \frac{1}{2}\frac{\rho}{F^2}\frac{\partial F}{\partial\rho}\frac{\partial F}{\partial z} - \frac{1}{2}\frac{F^2}{\rho}\frac{\partial\omega}{\partial\rho}\frac{\partial\omega}{\partial z}. \tag{2.5}$$

Then, γ can be found at any point in spacetime with an appropriate line integral. See Ref. [30], pp. 165–167 for further discussion. For our purposes, the main thing to note is that knowledge of $\mathcal{E}$—or equivalently $\tilde{\xi}$—specifies the *entire* spacetime metric.

The function $\tilde{\xi}$ can be expanded as

$$\tilde{\xi} = \sum_{j,k=0}^{\infty} a_{jk}\frac{\rho^j z^k}{(\rho^2+z^2)^{j+k}}. \tag{2.6}$$

The index j is strictly even. If k is even, a_{jk} is real; if k is odd, a_{jk} is imaginary. From these coefficients, it is relatively straightforward to extract the spacetime's multipole moments (M_l, S_l) using an algorithm developed by Fodor, Hoenselaers, and Perjés (FHP) [31]. By a recursive procedure that involves repeatedly differentiating $\tilde{\xi}$ and gathering terms,

FHP show that a_{jk} can be written in terms of the mass and current moments [see Ref. [24], Eqs. (35)–(41)]. For example, one can show that

$$a_{0l} = M_l + iS_l + \text{LOM}, \tag{2.7}$$

$$a_{l0} = (-1)^{l/2}\frac{(l-1)!!}{l!!}M_l + \text{LOM}, \tag{2.8}$$

$$a_{l-1,1} = i(-1)^{(l-1)/2}\frac{l!!}{(l-1)!!}S_l + \text{LOM}. \tag{2.9}$$

''LOM'' is an abbreviation for ''lower order moments:'' a complicated (but known) sum of various combinations of M_j and S_k with $j<l$ and $k<l$.

Ryan [24] uses the coefficients a_{jk} and their relationship to (M_l, S_l) as the basis for his spacetime mapping procedure. Since the spacetime is fully determined by a_{jk}, it follows that its orbits are likewise determined. An orbit in the spacetime (2.1) is governed by three orbital frequencies: Ω_ϕ, related to the time to cover 2π radians of azimuth; Ω_ρ, characterizing oscillations in the ρ coordinate; and Ω_z, for oscillations in the z coordinate. Ryan shows (via a power law expansion using orbital speed as an expansion parameter) how these frequencies depend on a_{jk}. Measurement of $(\Omega_\phi, \Omega_\rho, \Omega_z)$ (or accumulated phases associated with these frequencies) can therefore be used to measure a_{jk}. Ryan then inserts the measured values of a_{jk} into the FHP algorithm, determining the multipole moments of the spacetime. Using this procedure, Ryan showed that future gravitational-wave measurements with LISA should be able to determine enough moments to strongly constrain the black hole nature of massive compact objects [26].

Though sufficient to prove the principle, we believe that this procedure is not useful in practice for mapping the spacetimes of objects believed to be black holes. Referring to Eq. (2.6), we see that the coefficients a_{jk} are essentially labels for an expansion in inverse distance. For strong field orbits ($\rho, z \sim$ a few$\times M$), a large number of these coefficients must be kept in order to model the spacetime with sufficient accuracy. One might hope that the coefficients a_{jk} become small for large j and k, making it possible to truncate the expansion of $\tilde{\xi}$. This is not the case: because of the coupling to lower order moments [cf. Eqs. (2.7)–(2.9)], these coefficients generically remain large even if the body has only a small number of non-zero multipole moments.

In this language, the description of the spacetime and hence of its orbits becomes extremely complicated in the strong field. This makes testing whether a spacetime is close to that of a black hole very difficult. Naively, one might imagine requiring that a spacetime have the multipole moment structure

$$M_l + iS_l = M(ia)^l + \delta M_l + i\,\delta S_l, \tag{2.10}$$

and then developing a formalism similar to that described here to place observational limits on the deviations $(\delta M_l, \delta S_l)$. (Indeed, this how we originally conceived of this analysis.) One quickly discovers that the algebraic complexity associated with this approach is immense. Though no doubt possible in principle, a multipolar prescription like Eq. (2.10) does not easily translate into a *practical* scheme for constraining the properties of massive compact objects.

The lesson appears to be that multipoles, though conceptually clean and offering a beautiful description of weak-field gravity, simply are not the best tools in the strong field. This should not be surprising in a nonlinear theory like general relativity: since multipoles are basically labels in an inverse distance expansion (as we have repeatedly emphasized), a description that is clean in the weak field can easily turn into a mess when the nonlinearities are important.

III. BUILDING THE SPACETIME OF A BUMPY BLACK HOLE

Keeping in mind that the goal is just to build some candidate spacetime to be used as a straw man in testing the black hole hypothesis, we advocate a different approach. Our goal is to develop a family of spacetimes corresponding to stationary perturbed black holes: bumpy black holes. These spacetimes include black holes as a subset—we simply set the magnitude of the perturbation to zero. We construct these spacetimes in a manner that makes an exploration of its strong-field properties simple.

We will focus on axisymmetric spacetimes, in keeping with our goal of analyzing axisymmetric deformations of Kerr black holes. For this first analysis, we will further specialize to deformations of Schwarzschild black holes. Stationary, axisymmetric deformations of Schwarzschild black holes were in fact studied by SPR [29] with the goal of characterizing distortions to the event horizon. (Their analysis was a part of the ''Membrane Paradigm''; see Ref. [32].) Their calculation makes an ideal starting point for our analysis; the following discussion closely follows Ref. [29], Sec. III A.

As mentioned in the Introduction, the spacetimes we consider are described by the Weyl metric [28]:

$$ds^2 = -e^{2\psi}dt^2 + e^{2\gamma-2\psi}(d\rho^2 + dz^2) + e^{-2\psi}\rho^2 d\phi^2. \tag{3.1}$$

The vacuum Einstein equations for this line element reduce to

$$\frac{\partial^2\psi}{\partial\rho^2} + \frac{1}{\rho}\frac{\partial\psi}{\partial\rho} + \frac{\partial^2\psi}{\partial z^2} = 0, \tag{3.2}$$

$$\frac{\partial\gamma}{\partial\rho} = \rho\left[\left(\frac{\partial\psi}{\partial\rho}\right)^2 - \left(\frac{\partial\psi}{\partial z}\right)^2\right], \tag{3.3}$$

$$\frac{\partial\gamma}{\partial z} = 2\rho\frac{\partial\psi}{\partial\rho}\frac{\partial\psi}{\partial z}. \tag{3.4}$$

Equations (3.3) and (3.4) are identical to Eqs. (2.4) and (2.5) with $\omega = 0$ and $F = e^{2\psi}$. Note that Eq. (3.2) implies ψ is a

harmonic function in a fictitious Euclidean space with cylindrical coordinates ρ, z, and ϕ [29,30].

Following SPR [29], we observe that the function ψ is the Newtonian potential far from a source. A reasonable way to perturb ψ is by adding potential terms that correspond to particular mass distributions perturbing the background black hole; distributions that change the weak-field multipole structure of the hole are particularly interesting. [Note the linearity of Eq. (3.2)—*exact* solutions for ψ can be constructed by superposition.] We only require that the mass μ of the perturbations be small compared to the mass M of the black hole, allowing us to expand ψ and γ to first order.

Notice that, with our form of the perturbation, we expand in powers of μ/M, rather than $1/r$ (where r is some measure of distance from the source). The approximation we introduce should thus be well-behaved for any r, including into the strong field. Notice also that, because Eqs. (3.2)–(3.4) come from the *vacuum* Einstein equations, our metric will only hold where there is no matter. To perturb the background black hole, we will add matter in the form of point particles and one-dimensional rings. The metric will therefore not apply at the points containing that matter; it will in fact be singular at those locations. As long as we only examine regions of spacetime external to these perturbing sources, this singular behavior does not pose any difficulty.

For describing black holes, it is convenient to use prolate spheroidal coordinates u and v:

$$\rho = M \sinh u \sin v, \tag{3.5}$$

$$z = M \cosh u \cos v. \tag{3.6}$$

The coordinate $v \in [0,\pi]$ is a polar angle; $u \in [0,\infty)$ is effectively a radial coordinate. These coordinates cover the entire *exterior* Schwarzschild spacetime: the coordinate $u=0$ maps to the event horizon, $r=2M$ [cf. Eq. (3.15) below]. In the Weyl coordinates (ρ,z), this corresponds to a cylindrical rod at $\rho=0$ running from $z=-M$ to $z=M$.

The line element (3.1) becomes

$$ds^2 = -e^{2\psi}dt^2 + M^2 e^{2\gamma-2\psi}(\sinh^2 u + \sin^2 v)(du^2+dv^2) + M^2 e^{-2\psi}\sinh^2 u \sin^2 v \, d\phi^2. \tag{3.7}$$

We now put $\psi = \psi_0 + \psi_1$, $\gamma = \gamma_0 + \gamma_1$. We take the perturbations (ψ_1, γ_1) to be small compared to (ψ_0, γ_0):

$$\psi_1 \sim \frac{\mu}{M}\psi_0, \tag{3.8}$$

and likewise for γ. The Einstein equations constraining γ, Eqs. (3.3) and (3.4), become

$$\frac{\partial\gamma_1}{\partial u} = 2\rho^2 \cot v \left(\frac{\partial\psi_0}{\partial\rho}\frac{\partial\psi_1}{\partial z} + \frac{\partial\psi_0}{\partial z}\frac{\partial\psi_1}{\partial\rho} \right) + 2\rho z \tan v \left(\frac{\partial\psi_0}{\partial\rho}\frac{\partial\psi_1}{\partial\rho} - \frac{\partial\psi_0}{\partial z}\frac{\partial\psi_1}{\partial z} \right), \tag{3.9}$$

$$\frac{\partial\gamma_1}{\partial v} = 2\rho^2 \cot v \left(\frac{\partial\psi_0}{\partial\rho}\frac{\partial\psi_1}{\partial\rho} - \frac{\partial\psi_0}{\partial z}\frac{\partial\psi_1}{\partial z} \right) + 2\rho z \tan v \left(\frac{\partial\psi_0}{\partial\rho}\frac{\partial\psi_1}{\partial z} + \frac{\partial\psi_0}{\partial z}\frac{\partial\psi_1}{\partial\rho} \right). \tag{3.10}$$

We have only kept terms to leading order in the perturbation. It turns out that these two equations will *overdetermine* the solution (cf. [30], p. 167 for discussion). For our purposes, this means that we need integrate only one of them to determine γ_1 (up to a constant of integration). We will use Eq. (3.10); the solution we find also satisfies Eq. (3.9), as is easily verified by direct substitution.

At this point, we specialize our background to the Schwarzschild metric: we put [29]

$$\psi_0 = \ln \tanh u/2, \tag{3.11}$$

$$\gamma_0 = -\frac{1}{2}\ln\left(1 + \frac{\sin^2 v}{\sinh^2 u}\right). \tag{3.12}$$

Using Eqs. (3.11) and (3.12) and changing all instances of ρ,z to u,v as appropriate, Eq. (3.10) becomes

$$\frac{\partial\gamma_1}{\partial v} = \frac{2[\tan v(\partial\psi_1/\partial v) - \tanh u(\partial\psi_1/\partial u)]}{\sinh u(\coth u \tan v + \tanh u \cot v)}. \tag{3.13}$$

For completeness, the equation for $\partial\gamma_1/\partial u$ becomes

$$\frac{\partial\gamma_1}{\partial u} = \frac{2[\cot v(\partial\psi_1/\partial u) + \tanh u(\partial\psi_1/\partial v)]}{\sinh u(\coth u \tan v + \tanh u \cot v)}; \tag{3.14}$$

as already discussed, we will only focus on Eq. (3.13).

To solve for γ_1, we will first *impose* a particular ψ_1, taking advantage of the fact that ψ_1 can be thought of as a perturbation to the distant, Newtonian gravitational field of the black hole. We then integrate $\partial\gamma_1/\partial v$ with respect to v to find $\gamma_1(u,v)$, being careful to choose an appropriate integration constant by demanding that the perturbation vanish far from the black hole. The $\gamma_1(u,v)$ we find then automatically satisfies Eq. (3.9) or (3.14).

In preparation for these calculations, it is useful to put this metric into Schwarzschild-like form. Plugging Eqs. (3.11) and (3.12) into Eq. (3.7), and making the coordinate transformation [29]

$$r = 2M\cosh^2 u/2, \quad \theta = v \tag{3.15}$$

yields

$$ds^2 = -e^{2\psi_1}\left(1-\frac{2M}{r}\right)dt^2 + e^{2\gamma_1-2\psi_1}\left(1-\frac{2M}{r}\right)^{-1}dr^2 + r^2 e^{2\gamma_1-2\psi_1}d\theta^2 + r^2\sin^2\theta e^{-2\psi_1}d\phi^2. \tag{3.16}$$

Note that the transformation (3.15) implies

$$\rho = r \sin\theta \sqrt{1 - \frac{2M}{r}}, \tag{3.17}$$

$$z = (r - M)\cos\theta. \tag{3.18}$$

These relations can be particularly helpful when describing the perturbations in Schwarzschild coordinates.

Although the line element (3.16) is technically exact, in the following analysis we will only work to first order in the perturbation. We thus should really expand $e^{2\psi_1} \simeq 1 + 2\psi_1$, and likewise for γ_1. For compactness of notation, we leave these perturbations in the exponentials, with the caveat that they must be expanded to first order in all calculations.

Before examining some interesting perturbations, it is useful to carefully study orbits in this general perturbed spacetime. Several results can be found in terms of ψ_1 and γ_1, which facilitates later analysis. In the next section, we will examine the properties of equatorial orbits in this metric, and calculate the rate of periapse precession.

IV. EQUATORIAL ORBITS OF BUMPY BLACK HOLES

In this section, we study, as much as is possible, properties of bumpy black hole orbits that do not require specifying the perturbation. It is easy to find the geodesics in the equatorial plane ($\theta = \pi/2$); for this first analysis, we will focus on this simple case. It is not, in fact, difficult to generalize the equations of motion to orbits beyond the equatorial plane. To solve these equations, however, appears challenging: the equations for r and θ do not appear to separate in general (as they do, for example, in the Kerr case). We discuss this issue further in Sec. VIII.

As discussed in the Introduction, our goal is to understand how black hole bumpiness is imprinted upon measurable quantities—in particular, accumulated phases related to harmonics of the orbital frequencies. A simple (and historically important) effect is the shift of an orbit's periapsis. This shift is related to the mismatch between the r and ϕ frequencies. In the weak-field limit, it describes perihelion precession, well-known from studies of planetary orbits in our own solar system. In this section, we will derive a differential formula for the periapsis shift.

We begin by writing down a Lagrangian for orbiting bodies in this spacetime: put $\mathcal{L} = g_{ab}\dot{x}^a\dot{x}^b$ (where overdot denotes $d/d\tau$, with τ proper time along an orbit). Note that $\mathcal{L} = -1$. Since our focus here is equatorial orbits, we further put $\theta = \pi/2$ and $\dot{\theta} = 0$. (Thanks to the reflection symmetry, we are guaranteed that an equatorial trajectory remains equatorial.) The result is

$$\mathcal{L} = -e^{2\psi_1}\left(1 - \frac{2M}{r}\right)\dot{t}^2 + e^{2\gamma_1 - 2\psi_1}\left(1 - \frac{2M}{r}\right)^{-1}\dot{r}^2 + e^{-2\psi_1} r^2 \dot{\phi}^2. \tag{4.1}$$

Varying $\mathcal{L}$ with respect to t yields

$$\frac{d}{d\tau}\left[e^{2\psi_1}\left(1 - \frac{2M}{r}\right)\dot{t}\right] = 0, \tag{4.2}$$

leading us to identify the orbital energy per unit rest mass μ

$$E = e^{2\psi_1}\left(1 - \frac{2M}{r}\right)\dot{t} \tag{4.3}$$

as a constant of motion. By varying with respect to ϕ, we likewise identify the orbital angular momentum orthogonal to the equatorial plane per unit μ:

$$L = e^{-2\psi_1} r^2 \dot{\phi}. \tag{4.4}$$

An equation for the radial motion follows from $\mathcal{L} = -1$:

$$\dot{r}^2 = e^{-2\gamma_1}\left[E^2 - e^{2\psi_1}\left(1 - \frac{2M}{r}\right)\left(1 + \frac{e^{2\psi_1}L^2}{r^2}\right)\right]. \tag{4.5}$$

It is easy to see that this reduces to the usual Schwarzschild equation of motion for $\psi_1 = \gamma_1 = 0$ [compare, e.g., Ref. [10], Eq. (25.16a)]. For the calculations we will perform momentarily, it is useful to multiply this by r^3, defining

$$R(r) = r^3\dot{r}^2 = e^{-2\gamma_1}[(E^2 - e^{2\psi_1})r^3 + 2e^{2\psi_1}Mr^2 - e^{4\psi_1}L^2 r + 2e^{4\psi_1}L^2 M]. \tag{4.6}$$

Using $R(r)$, it is straightforward to remap the constants E and L to parameters that directly characterize the orbit. It is helpful to reparametrize r,

$$r = \frac{p}{1 + \varepsilon\cos\chi}. \tag{4.7}$$

As χ oscillates from 0 to π to 2π, the orbiting body moves from periapsis, $r_p = p/(1+\varepsilon)$, to apoapsis, $r_a = p/(1-\varepsilon)$, and back. In Newtonian gravity, this reparametrization facilitates identifying the orbits as closed ellipses; p is the orbit's semi-latus rectum and ε its eccentricity. This intuition remains very useful in general relativity, though the ellipses do not close—the time for χ to go from 0 to 2π is greater than the time for the orbit to move through 2π radians of azimuth ϕ.

The periapse and apoapse radii are the orbit's turning points. By definition, this means that $\dot{r}$ and hence $R(r)$ equal zero at these points. This makes it possible to find E and L as functions of p and ε: simultaneously solving $R(r_p) = 0$ and $R(r_a) = 0$ yields

$$E(p,\varepsilon)=e^{[\psi_1(r_p)+\psi_1(r_a)]}\sqrt{\frac{[(1+\varepsilon)^2e^{2\psi_1(r_p)}-(1-\varepsilon)^2e^{2\psi_1(r_a)}][p^2-4Mp+4M^2(1-\varepsilon^2)]}{p\{e^{4\psi(r_p)}(1+\varepsilon)^2[p-2M(1+\varepsilon)]-e^{4\psi(r_a)}(1-\varepsilon)^2[p-2M(1-\varepsilon)]\}}}, \tag{4.8}$$

$$L(p,\varepsilon)=p\sqrt{\frac{e^{2\psi(r_p)}[p-2M(1+\varepsilon)]-e^{2\psi(r_a)}[p-2M(1-\varepsilon)]}{e^{4\psi(r_p)}(1+\varepsilon)^2[p-2M(1+\varepsilon)]-e^{4\psi(r_a)}(1-\varepsilon)^2[p-2M(1-\varepsilon)]}}. \tag{4.9}$$

For orbits that are circular ($\varepsilon=0$), $r_p=r_a$, so the conditions $R(r_p)=0$, $R(r_a)=0$ do not provide separate information. In this case, we require $\partial R/\partial r=0$; this condition guarantees that $\dot{r}$ remains zero. Solving $R=0$, $\partial R/\partial r=0$ yields

$$E(p,\varepsilon=0)=e^{\psi_1(p)}\sqrt{\left(1-\frac{2M}{p}\right)\left[\frac{p-2M-p(p-2M)\partial\psi_1/\partial r}{p-3M-2p(p-2M)\partial\psi_1/\partial r}\right]}, \tag{4.10}$$

$$L(p,\varepsilon=0)=pe^{-\psi_1(p)}\sqrt{\frac{M+p(p-2M)\partial\psi_1/\partial r}{p-3M-2p(p-2M)\partial\psi_1/\partial r}}. \tag{4.11}$$

When the perturbation ψ_1 is set to zero, these expressions correctly reduce to formulas characterizing E and L for Schwarzschild black holes:

$$E(p,\varepsilon)=\sqrt{\frac{p^2-4Mp+4M^2(1-\varepsilon^2)}{p[p-M(3+\varepsilon^2)]}} \tag{4.12}$$

$$=\frac{1-2M/p}{\sqrt{1-3M/p}}\quad(\varepsilon=0); \tag{4.13}$$

$$L(p,\varepsilon)=p\sqrt{\frac{M}{p-M(3+\varepsilon^2)}} \tag{4.14}$$

$$=p\sqrt{\frac{M}{p-3M}}\quad(\varepsilon=0). \tag{4.15}$$

The function $R(r)$ also determines the parameters of the *last stable orbit*: solving the equation

$$\frac{\partial R}{\partial r}=0 \tag{4.16}$$

with $E=E(p,\varepsilon)$, $L=L(p,\varepsilon)$ determines a separatrix $p(\varepsilon)$ such that, at fixed eccentricity ε, orbits with $p<p(\varepsilon)$ are dynamically unstable. (For circular orbits, we must solve $\partial^2R/\partial r^2=0$.) The result is rather messy, so we do not present it explicitly. When the perturbation is turned off, the separatrix is simply given by $p=(6+2\varepsilon)M$.

We are now ready to derive a general formula for bumpy black hole periapsis precession. First, note that, via Eq. (4.7), the rate at which the orbital radius changes with respect to χ is

$$\frac{dr}{d\chi}=\frac{p\varepsilon\sin\chi}{(1+\varepsilon\cos\chi)^2}=\frac{r^2\varepsilon\sin\chi}{p}. \tag{4.17}$$

Combining Eqs. (4.4), (4.5), and (4.17), we find

$$\frac{d\phi}{d\chi}=\frac{d\phi}{d\tau}\frac{d\tau}{dr}\frac{dr}{d\chi}=e^{2\psi_1[r(\chi)]}e^{\gamma_1[r(\chi)]}L(p,\varepsilon)\varepsilon\sin\chi p^{-1}\times\left[E(p,\varepsilon)^2-e^{2\psi_1[r(\chi)]}\left[1-\frac{2M}{r(\chi)}\right]\right]\times\left[1+\frac{e^{2\psi_1[r(\chi)]}L(p,\varepsilon)^2}{r(\chi)^2}\right]^{-1/2}. \tag{4.18}$$

This equation expresses, in differential form, the amount of azimuth that accumulates per unit χ. Integrating $d\phi/d\chi$ over $0\leqslant\chi\leqslant2\pi$ gives the total accumulated azimuth in one full orbit. In Newtonian gravity, this number is 2π radians—Newtonian orbits are closed ellipses. The periapsis precession is the amount of "extra" azimuth that accumulates in one orbit:

$$\Delta\phi=\int_0^{2\pi}d\chi\frac{d\phi}{d\chi}-2\pi. \tag{4.19}$$

Having derived about as many orbital properties as we can in general, much of the rest of this paper will be devoted to integrating this equation with particular choices of the perturbing functions ψ_1 and γ_1. We turn now to a calculation of these perturbations and an exploration of their effects.

V. METRIC PERTURBATIONS I: POINT MASSES AT THE POLES

In this and the following section, we calculate the first-order metric perturbation in two special cases: a pair of point masses at the poles (this section), and a ring of mass about the equator (following section). These two perturbations are particularly interesting because they produce a quadrupolar distortion of the spacetime.

Point masses at the poles were analyzed by SPR in Ref. [29]. Their particular focus was on the perturbation at or near the hole's event horizon; we generalize their result to find the perturbation throughout the exterior spacetime.

We begin by choosing, in Weyl coordinates (t,ρ,z,ϕ), the ψ perturbation

$$\psi_1^{\rm NP}=-\frac{\mu/2}{\sqrt{\rho^2+(z-b)^2}}. \tag{5.1}$$

As described previously, this choice has a simple interpretation: adding a point mass to the system changes the Newtonian potential at infinity—ψ—by that of a point mass. Equation (5.1) describes a point with mass (as measured at infinity) $\mu/2$ at $z=b$, near the ''north'' pole. The corresponding ψ_1 for a perturbing mass near the ''south'' pole is

$$\psi_1^{\rm SP}=-\frac{\mu/2}{\sqrt{\rho^2+(z+b)^2}}. \tag{5.2}$$

The complete ψ perturbation is given by adding the contributions from the north and south poles.

Our choice for ψ_1 has a curious property: it corresponds to a nonspherical naked singularity at $\rho=0$, $z=\pm b$ (the Curzon solution [33]). One might object that a spacetime which includes such a singularity cannot be physical, since naked singularities are presumed, by cosmic censorship, not to exist in nature. Therefore, perhaps we should exclude such spacetimes from consideration.

As we have repeatedly emphasized, given the goals of this analysis, the physicality of our trial spacetime is irrelevant. We seek a family of spacetimes that we can compare with those found in nature. In particular, we need a family of spacetimes that deviate controllably and only slightly from black holes. For the purposes of uncovering whether a spacetime is a black hole or not, it makes no difference whether the deviations come from physics we expect or not. We merely want to set limits on the extent of any deviations that might exist.

Having specified ψ_1, we turn to the computation of γ_1. Focus first on the perturbation at the north pole. Switching to the prolate, spheroidal coordinates u and v, we rewrite

$$\psi_1^{\rm NP}=-\frac{\mu/2}{[M^2\sinh^2u\,\sin^2v+(b-M\cosh u\cos v)^2]^{1/2}}. \tag{5.3}$$

Insert this into Eq. (3.13):

$$\frac{\partial\gamma_1^{\rm NP}}{\partial v}=\frac{\mu M(b-M\cosh u\cos v)\sin v}{[M^2\sinh^2u\,\sin^2v+(b-M\cosh u\cos v)^2]^{3/2}},$$

$$=\frac{\mu}{M}\frac{(\hat b-\cosh u\cos v)\sin v}{[\sinh^2u\,\sin^2v+(\hat b-\cosh u\cos v)^2]^{3/2}}. \tag{5.4}$$

We have defined $\hat b=b/M$.

We now integrate this with respect to v to compute $\gamma_1^{\rm NP}$. Several manipulations help. First, simplify the denominator:

$$\begin{aligned}&\sinh^2u\,\sin^2v+(\hat b-\cosh u\cos v)^2\\&=\sinh^2u+\hat b^2-2\hat b\cosh u\cos v+\cos^2v\\&=(\cos v-\hat b\cosh u)^2+\hat b^2-\hat b^2\cosh^2u+\sinh^2u\\&=(\cos v-\hat b\cosh u)^2+(1-\hat b^2)\sinh^2u.\end{aligned} \tag{5.5}$$

Next, put $x=\cos v$, so $dx=-\sin v dv$:

$$\gamma_1^{\rm NP}=\frac{\mu}{M}\int\frac{(-\hat b+x\cosh u)dx}{[(x-\hat b\cosh u)^2+(1-\hat b^2)\sinh^2u]^{3/2}}. \tag{5.6}$$

Let $y=x-\hat b\cosh u$; $dy=dx$ (for these purposes u is fixed):

$$\begin{aligned}\gamma_1^{\rm NP}&=\frac{\mu}{M}\int\frac{(\hat b\sinh^2u+y\cosh u)dy}{[y^2+(1-\hat b^2)\sinh^2u]^{3/2}}\\&=\frac{\mu}{M}\left[\int\frac{y\cosh u\,dy}{[y^2+(1-\hat b^2)\sinh^2u]^{3/2}}\right.\\&\quad\left.+\int\frac{\hat b\sinh^2u dy}{[y^2+(1-\hat b^2)\sinh^2u]^{3/2}}\right].\end{aligned} \tag{5.7}$$

The first of these integrals is

$$\begin{aligned}&\int\frac{y\cosh u dy}{[y^2+(1-\hat b^2)\sinh^2u]^{3/2}}\\&=-\frac{\cosh u}{[y^2+(1-\hat b^2)\sinh^2u]^{1/2}}\\&=-\frac{\cosh u}{[\sinh^2u\,\sin^2v+(\hat b-\cosh u\cos v)]^{1/2}}.\end{aligned} \tag{5.8}$$

The second yields

$$\begin{aligned}&\int\frac{\hat b\sinh^2u dy}{[y^2+(1-\hat b^2)\sinh^2u]^{3/2}}\\&=\frac{y\hat b\sinh^2u}{[(1-\hat b^2)\sinh^2u][y^2+(1-\hat b^2)\sinh^2u]^{1/2}}\\&=\frac{\hat b}{1-\hat b^2}\frac{\cos v-\hat b\cosh u}{[\sinh^2u\,\sin^2v+(\hat b-\cosh u\cos v)^2]^{1/2}}.\end{aligned} \tag{5.9}$$

Restoring factors of M, the complete integral is

$$\gamma_1^{\rm NP} = \frac{\mu M(b\cos v - M\cosh u)}{(M^2-b^2)[M^2\sinh^2 u\sin^2 v + (b - M\cosh u\cos v)^2]^{1/2}}. \tag{5.10}$$

In these integrals, we have neglected integration constants that must now be determined. We do so by requiring that $\gamma^{\rm NP}$ go to zero at large radius, i.e. as $u\to\infty$. Our current form of the solution has

$$\gamma_1^{\rm NP}(u\to\infty) = -\frac{\mu M}{M^2-b^2}. \tag{5.11}$$

This is the value that must be subtracted to guarantee that $\gamma_1^{\rm NP}$ is well behaved at large radius. We thus finally obtain

$$\gamma_1^{\rm NP} = \left(\frac{\mu M}{M^2-b^2}\right) \times \frac{b\cos v - M\cosh u}{[M^2\sinh^2 u\sin^2 v + (b - M\cosh u\cos v)^2]^{1/2}} + \frac{\mu M}{M^2-b^2}. \tag{5.12}$$

To account for the south pole perturbation, we just add the perturbation with $b\to -b$. [Note that we do *not* add the south perturbation with an overall minus sign, as is done in Ref. [29]. That sign choice only holds for $u\ll 1$; see Ref. [29], discussion following Eq. (3.14). Note that this has no impact on our ability to study strong field orbits—the region $u\ll 1$ corresponds to a region just barely outside the event horizon, well inside of the last stable orbit.] By direct substitution, one can verify that this solution for γ_1 satisfies Eq. (3.9) as well.

The perturbed metric is now fully specified. For our purposes, it is very convenient to use Eq. (3.15) to convert to Schwarzschild coordinates. Doing so and defining the function

$$D(r,\theta,b) = (r^2 - 2Mr + b^2 + M^2\cos^2\theta - 2br\cos\theta + 2bM\cos\theta)^{1/2}, \tag{5.13}$$

the complete perturbations ψ_1 and γ_1 are

$$\psi_1 = -\frac{\mu}{2D(r,\theta,b)} - \frac{\mu}{2D(r,\theta,-b)}, \tag{5.14}$$

$$\gamma_1 = \frac{\mu M}{M^2-b^2}\left[\left(\frac{M + b\cos\theta - r}{D(r,\theta,b)}\right) + \left(\frac{M - b\cos\theta - r}{D(r,\theta,-b)}\right)\right] + \frac{2\mu M}{M^2-b^2}. \tag{5.15}$$

These expressions hold for all $r>2M$. Note the Schwarzschild coordinate locations of the point masses are $r=b+M$, $\theta=0,\pi$. We must choose $b>M$ in order for the perturbing masses to be in the hole's exterior.

Combining Eqs. (4.8), (4.9), (4.18), (4.19), (5.14), and (5.15), we can now calculate the periapse precession for equatorial orbits and the two-point-mass perturbation. Numerical results for the general, strong-field case will be discussed in Sec. VII B; here, we show the weak-field result ($p\gg M$, $p\gg b$). This weak-field phase shift breaks naturally into 3 pieces:

$$\Delta\phi^{\rm points} = \Delta\phi_{\rm Schw}(M+\mu) + \Delta\phi_{\rm anom}(\mu) + \Delta\phi_{\rm prol}(\mu,b), \tag{5.16}$$

where

$$\Delta\phi_{\rm Schw}(M+\mu) = \frac{6\pi(M+\mu)}{p} + \frac{3\pi(M^2+2M\mu)}{2p^2}(18+\varepsilon^2), \tag{5.17}$$

$$\Delta\phi_{\rm anom}(\mu) = -\frac{\pi\mu M}{p^2}(1+2\varepsilon^2), \tag{5.18}$$

$$\Delta\phi_{\rm prol}(\mu,b) = -\frac{3\pi\mu b^2}{Mp^2}. \tag{5.19}$$

These three pieces each have a simple physical explanation. The first, $\Delta\phi_{\rm Schw}$ is just the periapsis precession expected for a particle orbiting a Schwarzschild black hole with total mass $M+\mu$ (to leading order in μ, and to second order in $1/p$). The second, $\Delta\phi_{\rm anom}$, is an "anomalous" contribution to the precession arising from the fact that our perturbation is nonspherical and has non-zero total mass. As we show later, this term can be eliminated by appropriately designing the perturbing mass distribution.

The third piece, $\Delta\phi_{\rm prol}$, is the leading order contribution to the precession that arises from a prolate, quadrupolar distortion to the black hole. This term agrees exactly with a Newtonian calculation of periapse precession in the presence of a prolate quadrupolar distortion (cf. Appendix A).

VI. METRIC PERTURBATIONS II: AN EQUATORIAL RING

We next examine perturbations due to a circular, equatorial ring of mass μ about a black hole. Our procedure is essentially the same as that used in the two-point-mass example, though the form of the perturbing potential makes the calculation a bit more complicated. We choose for ψ_1 the potential of a ring with radius $\rho=b$ and total mass at infinity μ:

$$\psi_1^{\rm ring} = -\frac{\mu}{2\pi}\int_0^{2\pi}\frac{d\xi}{[\rho^2+z^2+b^2-2b\rho\cos\xi]^{1/2}}. \tag{6.1}$$

This potential can be re-expressed using the complete elliptic integral of the 1st kind; it turns out to be more convenient to leave it as written here.

Inserting this into Eq. (3.13) and integrating yields

$$\gamma_1^{\rm ring} = \int_0^{2\pi} d\xi \left[\mathcal{C}(\xi) - \frac{f(u,v,\xi)}{g(u,v,\xi)h(u,v,\xi)} \right], \qquad (6.2)$$

where

$$f(u,v,\xi) = \mu \cosh u (b^2 + M^2 \cosh^2 u - Mb \sinh u \sin v \cos\xi), \qquad (6.3)$$

$$g(u,v,\xi) = \pi[(M^2 + b^2\cos^2\xi)\cosh^2 u + b^2 \sin^2\xi], \qquad (6.4)$$

$$h(u,v,\xi) = (M^2 \sinh^2 u \sin^2 v + M^2 \cosh^2 u \cos^2 v + b^2 - 2Mb \sinh u \sin v \cos\xi)^{1/2}. \qquad (6.5)$$

The integration "constant" $\mathcal{C}(\xi)$ is chosen, as in the two-point-mass case, to make γ_1 vanish at large distances. It has the value

$$\mathcal{C}(\xi) = \frac{\mu M}{\pi(M^2 + b^2\cos^2\xi)}. \qquad (6.6)$$

To evaluate the periapsis precession, it is useful to have these results in Schwarzschild coordinates. Using Eq. (3.15), f, g, and h become

$$f(r,\theta,\xi) = \frac{\mu}{M}(r-M)[b^2 + (r-M)^2 - b\sqrt{r^2 - 2Mr}\sin\theta\cos\xi], \qquad (6.7)$$

$$g(r,\theta,\xi) = \pi\left[\left(1 + \frac{b^2}{M^2}\cos^2\xi \right)(r-M)^2 + b^2\sin^2\xi \right], \qquad (6.8)$$

$$h(r,\theta,\xi) = [(r^2 - 2Mr)\sin^2\theta + (r-M)^2\cos^2\theta + b^2 - 2b\sqrt{r^2-2Mr}\sin\theta\cos\xi]^{1/2}. \qquad (6.9)$$

The ring's radius in Schwarzschild coordinates is $r = M + \sqrt{M^2 + b^2}$; any choice $b > 0$ will produce a ring in the hole's exterior.

Since the integration over ξ commutes with other operations (notably expanding for large p) it is straightforward to combine Eqs. (4.8), (4.9), (4.18), (4.19), (6.1), and (6.2) to compute the periapsis precession in this spacetime. We do so numerically in Sec. VII B; for now, we evaluate the weak-field precession ($p \gg M$, $p \gg b$):

$$\Delta\phi^{\rm ring} = \Delta\phi_{\rm Schw}(M+\mu) + \Delta\phi_{\rm anom}(\mu) + \Delta\phi_{\rm obl}(\mu,b). \qquad (6.10)$$

The terms $\Delta\phi_{\rm Schw}(M+\mu)$ and $\Delta\phi_{\rm anom}(\mu)$ are defined in Eqs. (5.17) and (5.18); they are identical to the corresponding terms for the point mass perturbations. The term

$$\Delta\phi_{\rm obl}(\mu,b) = +\frac{3\pi\mu b^2}{2Mp^2} \qquad (6.11)$$

gives the contribution to the precession due to an *oblate* quadrupolar distortion to the black hole. As in the prolate case, this term agrees exactly with a Newtonian calculation of periapse precession presented in Appendix A.

VII. METRIC PERTURBATIONS III: PURE QUADRUPOLE PERTURBATION

A. Weak-field analysis

Each of our perturbations changed not only the quadrupole ($l=2$) structure of the spacetime, but the spacetime's total mass ($l=0$) as well. To construct a perturbation that is purely quadrupolar (at least in the weak field), we take advantage of the linearity of the perturbed Einstein equations to superpose a ring of mass $\pm\mu$ with a pair of points of mass $\mp\mu/2$ each. A negative mass perturbation may seem strikingly unphysical, but as discussed in Sec. III, our goal is not to build perturbations that are likely to exist in nature. (Given the naked singularity interpretation, it is arguable that a negative mass perturbation is no less physical than one of positive mass.)

From now on, we will focus on this zero-mass perturbation. The weak field result periapse precession for this case is

$$\Delta\phi^{\rm both} = \Delta\phi_{\rm Schw}(M) + \Delta\phi_{\rm quad}(\mu,b), \qquad (7.1)$$

where the quadrupole contribution is

$$\Delta\phi_{\rm quad}(\mu,b) = \pm\frac{9\pi\mu b^2}{2Mp^2}. \qquad (7.2)$$

Notice that the "anomalous" contribution to the precession does not appear in this case. Making the perturbation have zero mass apparently suffices to eliminate that term. What remains is a periapsis precession term corresponding to a *purely quadrupolar* deformation of the spacetime. We have succeeded in constructing a spacetime that is *almost* that of a black hole, that is good deep into the strong field, but has one multipole moment—M_2—with the "wrong" value.

B. Strong-field analysis

Having demonstrated that our calculations match up in a sensible way with Newtonian and relativistic calculations of periapse precession, we now show numerical calculations for the strong fields of bumpy black holes. In all of our figures and discussion, our focus is on the precession induced *relative to* periapsis precession for a normal black hole. To help calibrate the effect that the bumpiness has, we show in Fig. 1 the periapsis precession $\delta\phi$ (the amount of azimuth ϕ accumulated in one orbit, minus 2π) in the strong field of a

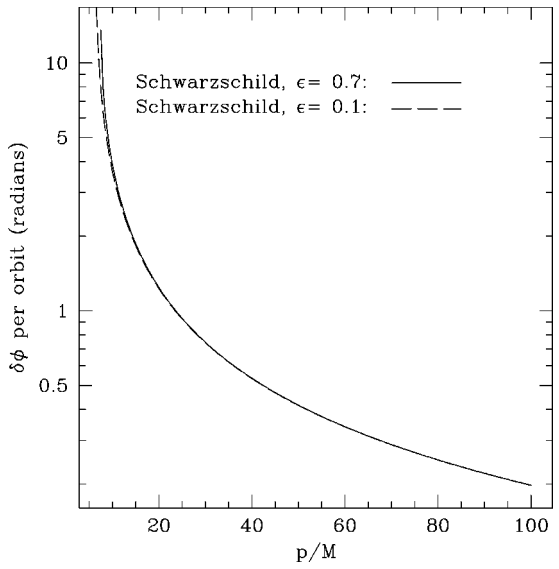

FIG. 1. Periapsis precession in the strong field of a Schwarzschild black hole: the ''extra'' azimuth accumulated over a single orbit with parameters (p,ε). The solid curve is for eccentricity $\varepsilon=0.7$; the dashed one is for $\varepsilon=0.1$. As we go to the weak field, $\delta\phi$ approaches zero—orbits approach closed ellipses. The degree of precession is large in the strong field: the limiting value ~ 12 radians corresponds to almost 2 extra revolutions around the symmetry axis.

Schwarzschild black hole. Notice that $\delta\phi$ becomes quite large in the strong field, corresponding to almost 2 extra revolutions around the hole.

Figures 2 and 3 show the shift $\Delta\phi$ associated with two different choices of bumpiness. In both plots, we have put $\mu/M=0.01$; since the Einstein equations and the equations of motion all scale linearly with μ, $\Delta\phi$ is likewise linear in

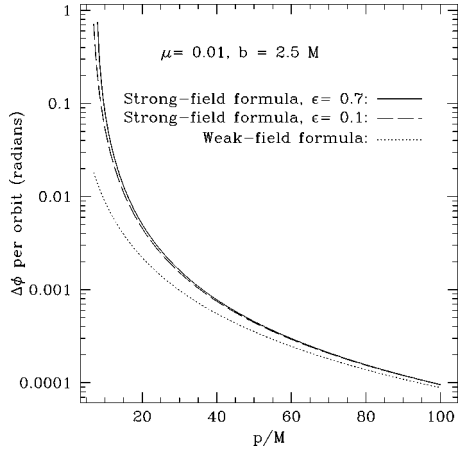

FIG. 2. Periapsis precession in the strong field of a bumpy black hole: the ''extra'' azimuth accumulated due to the hole's bumpiness as a function of (p,ε). We have put $\mu/M=0.01$ and $b=2.5M$. By the linearity of all relevant equations in mass, the degree of precession scales proportional to μ. The solid curve is for $\varepsilon=0.7$; the dashed one is for $\varepsilon=0.1$. The dotted curve shows the weak-field prediction. Both strong-field results asymptotically approach the weak-field prediction for large p.

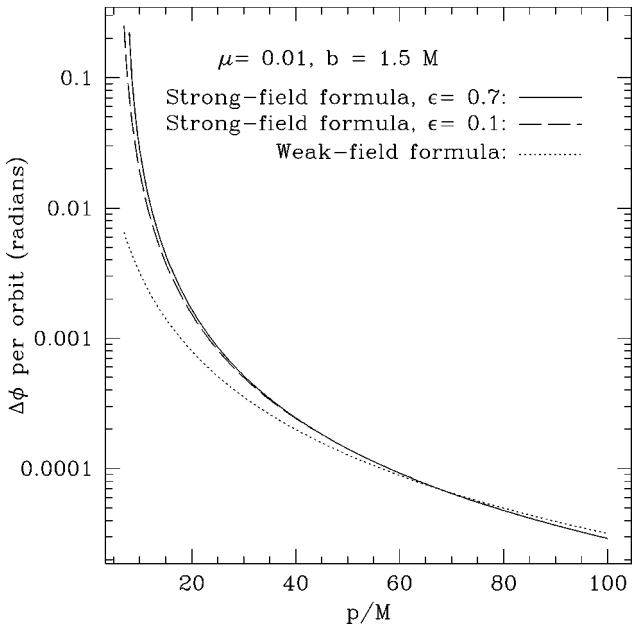

FIG. 3. Periapsis precession in the strong field of a bumpy black hole: the ''extra'' azimuth accumulated due to the hole's bumpiness as a function of (p,ε). This plot is identical to Fig. 2 except that we have put $b=1.5M$.

μ. Thus, it is a simple matter to rescale to other masses. We examine strong-field precession for $\varepsilon=0.7$ and $\varepsilon=0.1$ in these plots; we also compare these results to the weak-field prediction (7.2).

Several features are evident. First, in both cases, the strong-field results asymptotically approach the weak-field formula for large p—an important sanity check. Interestingly, as b is increased from $1.5M$ to $2.5M$, the weak-field formula changes from overestimating the periapsis shift to underestimating it. This behavior may be due to deviations of our potential from that of a perfect quadrupole. Second, at most orbits, the eccentricity has very little impact on this shift, at least for the values we examine. This is not surprising; the bare Schwarzschild periapsis precession (Fig. 1) is likewise fairly insensitive to the eccentricity. Finally, even into the strong field, the periapsis shift scales approximately with b^2 (the weak-field prediction). We can thus regard $\mu b^2/M^3$ as a measurable, dimensionless ''bumpiness parameter'' for the black hole.

Most interesting is the robustness with which the quadrupolar bump is manifested in the periapsis result: the effect is quite pronounced in the strong field. Indeed, the weak-field prediction (7.2) underestimates the degree of precession due to the hole's bumpiness by a factor ~ 3 over much of the strong field (~ 10 as we approach the last stable orbits). Over much of the strong field, the effect is large enough that, by observing over multiple orbital cycles, we should be able to set very interesting limits on the bumpiness of black hole candidates. For example, at $p\sim 20M$, the periapsis shift per orbit is roughly

$$\Delta\phi \simeq 10^{-3}\left(\frac{\mu b^2/M^3}{0.02}\right). \tag{7.3}$$

A bumpiness $\mu b^2/M^3 \simeq 0.02$ should thus be easily measurable after tracking roughly 1000 orbits (corresponding to when the bump shifts the accumulated phase by about 1 radian). Conversely, tracking the phase for N orbital cycles at this value of p should make it possible to constrain the bumpiness to be

$$\frac{\mu b^2}{M^3} \lesssim \frac{20}{N}. \tag{7.4}$$

Better limits can be obtained for orbits at smaller p.

Obviously, more detailed work is needed to carefully examine how well black hole bumpiness can be measured in a variety of scenarios (akin to Ryan's analysis of multipole measurability by LISA, Ref. [26]). But, these results suggest that measurements which coherently follow orbital phases—such as gravitational-wave measurements and x-ray timing—should be able to place *stringent* constraints on the bumpiness of black hole candidates. Bumpy black holes should thus be very useful tools in designing a formalism to map the strong field structure of black hole candidates in nature.

VIII. CONCLUSION

In this paper, we have laid the foundations for a null experiment to test whether a massive compact object is a black hole. The bumpy black hole spacetimes we construct differ only slightly from normal black hole spacetimes; and, the difference is controlled by a simple adjustable parameter—the hole's ''bumpiness.'' It should be possible to compare the properties of black hole candidates in nature with these bumpy black hole spacetimes. If these objects are in fact the black holes of general relativity, measurements will show that the natural spacetimes have a bumpiness of zero.

Quite a bit more work is needed in order to make the bumpy black hole concept useful in practice for astrophysical measurements:

Foremost is the need to generalize this analysis to bumpy Kerr black holes—zero angular momentum is a highly unrealistic idealization. In Appendix B, we show how, by choosing ψ, γ, and using an appropriate coordinate transformation, the Weyl metric (3.1) encompasses Kerr black holes (in Boyer-Lindquist coordinates). There should then be no severe difficulty perturbing this metric to build bumpy Kerr black holes, though the details are likely to be complicated.

Probably next in importance is generalizing the orbits which we analyze to include inclination with respect to the hole's equatorial plane. Besides the astrophysical motivation—we do not often expect orbits to be confined to a special plane—the inclusion of an extra degree of orbital freedom offers opportunity. Motions out of the plane are characterized by oscillations with a frequency Ω_θ which is generically different from the frequencies Ω_ϕ and Ω_r discussed in this paper. These oscillations thus offer an additional ''handle'' by which deviations from the black hole spacetime can be characterized.

As already mentioned in Sec. IV, the equations of motion for inclined orbits of bumpy black holes do not appear to separate (as they do for normal Kerr black holes). However, the fact that, by definition, bumpy black hole spacetimes are *nearly* the spacetimes of black holes suggests that the equations of motion must *nearly* separate. In other words, the degree to which the θ motion couples to the r and ϕ motion must be small—no doubt controlled by a coupling factor that is of order μ/M. It may be possible to take advantage of this smallness to usefully describe inclined and eccentric bumpy black hole orbits.

We have focused on perturbing mass distributions that produce, in the weak field, a purely quadrupolar spacetime distortion. We chose to focus on this case because an incorrect quadrupole moment is sufficient to falsify the black hole hypothesis. There is no reason why we could not go beyond this: by using rings out of the hole's equatorial plane, one could imagine building essentially any multipolar distribution whatsoever. Indeed, the fact that the equation for the metric function ψ in Weyl coordinates [Eq. (3.2)] is simply $\nabla^2\psi = 0$ tells us that it is simple in principle to specify perturbations whose weak-field multipolar structure is completely arbitrary: the perturbation

$$\psi_1 = \sum \frac{\mathcal{B}_l Y_{l0}}{(\rho^2+z^2)^{(l+1)/2}} \tag{8.1}$$

will work perfectly. The parameter $\mathcal{B}_l$ is a generalized l-polar ''bumpiness.'' With this ansatz to define our deviations, we can build bumpy black holes with almost arbitrarily shaped bumps. This will make it possible to strongly constrain the properties of black holes in nature.

As this paper was being completed, an analysis appeared on the gr-qc archive by Ashtekar et al. [35] of the multipole moments of isolated horizons [36]. Although we have not investigated this in any depth, it may be beneficial to pursue a connection between the bumpiness of a black hole and the multipole moments expressed in the language of Ref. [35].

Finally, it will be necessary to understand what impact the local environment may have on the bumpiness of a black hole candidate. Astrophysical black holes will be distorted, even if only slightly, by matter in their vicinity—for example, accreting material, orbiting bodies, and the galactic potential in which they are embedded. The real universe is not clean and asymptotically flat! In thinking about actual applications of this formalism, it will be important to understand what level of ''bumpiness'' can be expected.

With these generalizations in hand, it should be possible to begin examining detailed mechanisms by which orbital frequencies can be imprinted on astrophysical observables. For example, one can imagine analyzing accretion disk models to see how a spacetime's bumpiness is imprinted on quasi-periodic oscillations in a source's x-ray spectrum [13,37,38]. Another example is in gravitational-wave science. For these ideas to be useful for testing the nature of black hole candidates, we will need to model the gravitational-wave emission and inspiral of small compact bodies captured by bumpy black holes. This problem may not be much more difficult than the corresponding problem for normal Kerr black holes—because the wave amplitude is itself perturbatively small, the inspiral and wave generation

should decouple (at least to first order) from the spacetime's bumps. We hope to address at least some of these issues in future work.

ACKNOWLEDGMENTS

We thank Deepto Chakrabarty, Éanna Flanagan, and Emanuele Berti for useful discussions. The package MATHEMATICA was used to aid some of the calculations, particularly the weak-field expansions. This work was supported by NASA Grant NAG5-12906 and NSF Grant PHY-0244424.

APPENDIX A: PERIAPSE PRECESSION IN NEWTONIAN THEORY

An elliptical orbit precesses even in Newtonian gravity if the orbit is about a body with a quadrupole moment. Here, we calculate this precession, presenting results in a form useful for making contact with this paper's relativistic results.

A body with a mass and a quadrupole moment has a Newtonian gravitational potential

$$\Phi = -\frac{M}{r} - \frac{3}{2}\frac{\mathcal{I}_{ab}n^a n^b}{r^3}. \tag{A1}$$

For further discussion, see Thorne's voluminous treatise on multipole moments in general relativity [34]. The tensor $\mathcal{I}_{ab}$ is the symmetric, trace-free quadrupole moment of the gravitating source:

$$\mathcal{I}_{ab} = \int d^3r\rho\left(x_a x_b - \frac{1}{3}\delta_{ab}r^2\right). \tag{A2}$$

The vector n^a is a direction cosine. For notational simplicity, we put $\mathcal{I}_{ab}n^a n^b \equiv Q$.

A body in an equatorial orbit around this object obeys a simple equation of motion:

$$\left(\frac{dr}{dt}\right)^2 = E - \Phi - \frac{L^2}{2r^2}$$

$$\equiv \frac{R_{\rm newt}(r)}{r^3}, \tag{A3}$$

where L is the component of orbital angular momentum perpendicular to the equatorial plane. We are interested in eccentric orbits, so we reparametrize in the usual way:

$$r = \frac{p}{1+\varepsilon\cos\chi}, \tag{A4}$$

which is equivalent to

$$u = v(1+e\cos\chi) \tag{A5}$$

with $u = 1/r$, $v = 1/p$. The turning points of an eccentric orbit are at apoapsis, $u_a = v(1-\varepsilon)$, and periapsis, $u_p = v(1+\varepsilon)$. Solving the equation of motion at both turning points—$R_{\rm newt}(u_a) = 0$, $R_{\rm newt}(u_p) = 0$—yields a solution for the energy E and angular momentum L as functions of v and ε:

$$E = \frac{1}{2}(\varepsilon^2-1)Mv + \frac{3}{4}(\varepsilon^2-1)^2 Qv^3, \tag{A6}$$

$$L^2 = \frac{M}{v} + \frac{3}{2}(3+\varepsilon^2)Qv. \tag{A7}$$

An orbit corresponds to moving through the range $\chi = 0$ to $\chi = 2\pi$. We want to find the amount of azimuthal angle ϕ that accumulates over that orbit; that number (minus 2π) is the accumulated periapsis precession. First, use the above results for E and L in the radial equation of motion:

$$\left(\frac{dr}{dt}\right)^2 = \frac{1}{2}\varepsilon^2 v\sin^2\chi[2M + 3(\varepsilon^2-3)Qv^2 - 6\varepsilon Qv^2\cos\chi]. \tag{A8}$$

Next, using $r = 1/[v(1+\varepsilon\cos\chi)]$ we have

$$\frac{dr}{dt} = r^2\varepsilon v\sin\chi\frac{d\chi}{dt}. \tag{A9}$$

We obtain

$$\left(\frac{d\chi}{dt}\right)^2 = \frac{2M + 3(\varepsilon^2-3)Qv^2 - 6\varepsilon Qv^2\cos\chi}{2vr^4}. \tag{A10}$$

We leave the r^4 in the denominator to cancel another factor that will appear shortly.

To connect this to the azimuthal angle ϕ, we use the fact that $L = r^2 d\phi/dt$. Combining this with Eq. (A10), we obtain an equation for the differential periapsis advance:

$$\left(\frac{d\phi}{d\chi}\right)^2 = \left(\frac{d\phi}{dt}\right)^2\left(\frac{d\chi}{dt}\right)^{-2}$$

$$= \left(\frac{L}{r^2}\right)^2\left[\frac{2vr^4}{2M + 3(\varepsilon^2-3)Qv^2 - 6\varepsilon Qv^2\cos\chi}\right]$$

$$= \frac{2M + 3(3+\varepsilon^2)Qv^2}{2M + 3(\varepsilon^2-3)Qv^2 - 6\varepsilon Qv^2\cos\chi}. \tag{A11}$$

We now take the square root. We assume that $Qv^2 \equiv Q/p^2 \ll M$ and expand in v. This amounts to a weak field expansion. We find, to leading order in Qv^2/M,

$$\frac{d\phi}{d\chi} = 1 + \frac{3Qv^2(3+\varepsilon\cos\chi)}{2M}. \tag{A12}$$

Integrating over an orbit yields

$$\Delta\phi = \int_0^{2\pi} d\chi\frac{d\phi}{d\chi} - 2\pi = \frac{9\pi Qv^2}{M}. \tag{A13}$$

We now compute Q for the cases examined in the text: two point masses on the symmetry axis, and an equatorial

ring. The direction cosines are easy to calculate; we are only interested in orbits on the equatorial plane, so $n^z=0$. By axisymmetry, all directions in the equatorial plane are equivalent, so we choose $n^x=1$, $n^y=0$. Then, $Q=\mathcal{I}_{xx}$.

For a point mass $\mu/2$ at the north pole,

$$\mathcal{I}_{ab}^{\rm NP}=\frac{\mu b^2}{6}\,{\rm diag}(-1,-1,2); \tag{A14}$$

for a point mass at the south pole, we find the same result. The pair of point masses thus has $Q=-\mu b^2/3$. Using this Q in Eq. (A13) we find

$$\Delta\phi^{\rm points}=-\frac{3\pi\mu b^2}{p^2 M}. \tag{A15}$$

Repeating this exercise for the ring, we find

$$\mathcal{I}_{ab}^{\rm ring}=\frac{\mu b^2}{6}\,{\rm diag}(1,1,-2), \tag{A16}$$

so $Q=\mu b^2/6$, and

$$\Delta\phi^{\rm ring}=+\frac{3\pi\mu b^2}{2p^2 M}. \tag{A17}$$

Notice that $\Delta\phi^{\rm points}=-2\Delta\phi^{\rm ring}$. This follows from the spherical harmonics that describe the ring $[Y_{20}(\pi/2)]$ and the point masses $[Y_{20}(0)=-2Y_{20}(\pi/2)]$.

APPENDIX B: THE KERR METRIC FROM THE WEYL METRIC

In this appendix, we lay out the coordinate transformations and the choices of ψ and γ needed to go from the Weyl metric to the Kerr metric in Boyer-Lindquist coordinates. Although only the uncharged version is astrophysically relevant, we show the results for general charge Q. This calculation shares much with the Newman-Janis algorithm [39–41].

We begin with the Weyl metric in prolate spheroidal coordinates, Eq. (3.7). We then choose

$$M\cosh u=r-M+i\sqrt{a^2+Q^2}. \tag{B1}$$

Note that u must be complex; the black hole parameters M, a, and Q, as well as the radial coordinate r are of course real. As we discuss further below, this implies a severe constraint on the values u may take in the complex plane.

It follows that

$$\begin{aligned} dr&=M\sinh u\,du,\\ M^2\cosh^2 u&\equiv M^2|\cosh u|^2\\ &=(r-M)^2+a^2+Q^2,\\ M^2\sinh^2 u&=r^2-2Mr+a^2+Q^2. \end{aligned} \tag{B2}$$

We also choose $v=\theta$. For notational convenience, define

$$\begin{aligned} \Delta&=r^2-2Mr+a^2+Q^2,\\ \Sigma&=r^2+a^2\cos^2\theta. \end{aligned} \tag{B3}$$

Substituting into the metric (3.7), we find

$$\begin{aligned} ds^2=&-e^{2\psi}dt^2+e^{2\gamma-2\psi}\left(\frac{\Delta+M^2\sin^2\theta}{\Delta}\right)dr^2\\ &+e^{2\gamma-2\psi}(\Delta+M^2\sin^2\theta)\,d\theta^2+e^{-2\psi}\Delta\sin^2\theta\,d\phi^2. \end{aligned} \tag{B4}$$

Next, choose

$$\begin{aligned} e^{2\psi}&=\frac{\Delta}{\Sigma},\\ e^{2\gamma}&=\frac{\Delta}{\Delta+M^2\sin^2\theta}, \end{aligned} \tag{B5}$$

and put

$$\begin{aligned} dt&=dt'-a\sin^2\theta\,d\phi',\\ d\phi&=\frac{(r^2+a^2)}{\Sigma}d\phi'-\frac{a}{\Sigma}dt'. \end{aligned} \tag{B6}$$

Dropping the primes on t and ϕ, we see that the Weyl metric reduces to the Kerr-Newman metric in Boyer-Lindquist coordinates:

$$\begin{aligned} ds^2=&-\frac{\Delta}{\Sigma}(dt-a\sin^2\theta\,d\phi)^2+\frac{\sin^2\theta}{\Sigma}[(r^2+a^2)d\phi-a\,dt]^2\\ &+\frac{\Sigma}{\Delta}dr^2+\Sigma\,d\theta^2. \end{aligned} \tag{B7}$$

Compare, for example Ref. [10], Eq. (33.2) and Ref. [30], Eq. (12.3.1).

In prolate spheroidal coordinates, the functions ψ and γ are given by

$$e^{2\psi}=\frac{M^2\cosh^2 u}{r^2(u)+a^2\cos^2 v}, \tag{B8}$$

$$e^{2\gamma}=\frac{M^2\cosh^2 u}{M^2\cosh^2 u+M^2\sin^2 v}, \tag{B9}$$

where

$$r(u)=M(\cosh u-1)-i\sqrt{a^2+Q^2}. \tag{B10}$$

The requirement that $r(u)$ be real implies a severe constraint between the real and imaginary parts of u: we must have $\mathrm{Im}(M\cosh u)=+i\sqrt{a^2+Q^2}$. Writing $u=u_r+iu_i$, we find

$$M\sin(u_i)\sinh(u_r)=+\sqrt{a^2+Q^2}. \tag{B11}$$

In other words, u cannot take just any value in the complex plane, but must be confined to the trajectory defined by Eq. (B11).

Using these results, it should straightforward to generalize our calculations to describe bumpy Kerr black holes.

[1] J. Kormendy and D. Richstone, Annu. Rev. Astron. Astrophys. **33**, 581 (1995).

[2] J. Kormendy, to appear in the Carnegie Observatories Astrophysics Series, Vol. 1, edited by L.C. Ho; astro-ph/0306353.

[3] C.D. Bailyn, R.K. Jain, P. Coppi, and J.A. Orosz, Astrophys. J. **499**, 367 (1998).

[4] M.C. Miller and E.J.M. Colbert, Int. J. Mod. Phys. D **13**, 1 (2004).

[5] M. Colpi, S.L. Shapiro, and I. Wasserman, Phys. Rev. Lett. **57**, 2485 (1986).

[6] F.D. Ryan, Phys. Rev. D **55**, 6081 (1997).

[7] P.O. Mazur and E. Mottola, gr-qc/0109035.

[8] G. Chapline, E. Hohlfield, R.B. Laughlin, and D.I. Santiago, Philos. Mag. B **81**, 235 (2001).

[9] This statement assumes that the compact object in question rotates. By Birkhoff's theorem (e.g., Ref. [10], pp. 843, 844), an object with precisely zero angular momentum has an external spacetime identical to the exterior of a nonrotating black hole. Since all macroscopic astrophysical objects have at least some angular momentum, Birkhoff's theorem is not relevant.

[10] C.W. Misner, K.S. Thorne, and J.A. Wheeler, *Gravitation* (Freeman, San Francisco, 1973).

[11] A.M. Ghez, M. Morris, E.E. Becklin, A. Tanner, and T. Kremenek, Nature (London) **407**, 349 (2000).

[12] A. Eckart, R. Genzel, T. Ott, and R. Schödel, Mon. Not. R. Astron. Soc. **331**, 917 (2002).

[13] D. Psaltis, Adv. Space Res. **28**, 481 (2001).

[14] S.A. Hughes, Ann. Phys. (N.Y.) **303**, 142 (2003).

[15] L. Barack and C. Cutler, Phys. Rev. D **69**, 082005 (2004).

[16] M.J. Rees, in *Future of Theoretical Physics and Cosmology: Celebrating Stephen Hawking's 60th Birthday*, edited by G.W. Gibbons, E.P.S. Shellard, and S.J. Rankin (Cambridge University Press, Cambridge, England, 2003), pp. 217–235.

[17] R. Geroch, J. Math. Phys. **11**, 2580 (1970).

[18] R.O. Hansen, J. Math. Phys. **15**, 46 (1974).

[19] B. Carter, Phys. Rev. Lett. **26**, 331 (1971).

[20] D.C. Robinson, Phys. Rev. Lett. **34**, 905 (1975).

[21] R.H. Price, Phys. Rev. D **5**, 2419 (1972).

[22] R.H. Price, Phys. Rev. D **5**, 2439 (1972).

[23] The name ''bothrodesy'' was coined by Sterl Phinney during a talk given at Caltech in June 2001. This term descends from the use by Brandon Carter, Martin Rees, Steinn Sigurdsson, and various collaborators of the root ''bothros'' to describe properties of black holes; e.g., closest approach in an orbit is ''peribothron.'' This root in turn comes from ''$\beta o\theta\rho o\varsigma$,'' which in ancient Greek meant a sacrificial pit—a fitting association for black holes. Unfortunately, this word has rather less savory connotations in modern Greek, translating roughly to ''sewage pit.'' The phrase ''holiodesy'' was suggested by Marc Favata as a suitable replacement, incorporating the root ''hole'' and making a nice pun on ''heliodesy'' (measurement of the Sun's multipole moments via orbits).

[24] F.D. Ryan, Phys. Rev. D **52**, 5707 (1995).

[25] http://lisa.nasa.gov

[26] F.D. Ryan, Phys. Rev. D **56**, 1845 (1997).

[27] The multipole expansion turns out to be quite useful in the moderately strong field of some compact objects—cf. application of this expansion to accretion disks of a neutron star: M. Shibata and M. Sasaki, Phys. Rev. D **58**, 104011 (1998).

[28] H. Weyl, Ann. Phys. (Leipzig) **54**, 117 (1918).

[29] W.-M. Suen, R.H. Price, and I.H. Redmount, Phys. Rev. D **37**, 2761 (1988).

[30] R.M. Wald, *General Relativity* (University of Chicago Press, Chicago, 1984).

[31] G. Fodor, G. Hoenselaers, and Z. Perjés, J. Math. Phys. **30**, 2252 (1989).

[32] K.S. Thorne, R.H. Price, and D.A. MacDonald, *Black Holes: The Membrane Paradigm* (Yale University Press, New Haven, 1986).

[33] H.E.J. Curzon, Proc. London Math. Soc. **23**, 477 (1924).

[34] K.S. Thorne, Rev. Mod. Phys. **52**, 299 (1980).

[35] A. Ashtekar, J. Engle, T. Pawlowski, and C. van den Broeck, gr-qc/0401114.

[36] A. Ashtekar, C. Beetle, O. Dreyer, S. Fairhurst, B. Krishnan, J. Lewandowski, and J. Wisniewski, Phys. Rev. Lett. **85**, 3564 (2000).

[37] J.D. Schnittman and E. Bertschinger, astro-ph/0309458.

[38] L. Rezzolla, to appear in Proceedings of X-ray Timing 2003: Rossi and Beyond, edited by P. Kaaret, F.K. Lamb, and J.H. Swank; astro-ph/0401078.

[39] E.T. Newman and A.I. Janis, J. Math. Phys. **6**, 915 (1965).

[40] E.T. Newman, E. Couch, K. Chinnapared, A. Exton, A. Prakash, and R. Torrence, J. Math. Phys. **6**, 918 (1965).

[41] S.P. Drake and P. Szekeres, Gen. Relativ. Gravit. **32**, 445 (2000); also gr-qc/9807001.